Contents

1 Neutrino oscillations, and the evidence for neutrino masses and mixings 1

1.1 Neutrinos and the weak interactions: a historical perspective 1

1.2 Theory of massless and massive neutrinos 6

1.2.1 Massless neutrinos and the Standard Model 6

1.2.2 The see-saw mechanism for massive neutrinos 8

1.3 Neutrino mixing and flavor oscillations 10

1.4 Experimental signatures for neutrino oscillations 14

1.4.1 Atmospheric neutrino oscillations 15

1.4.2 Solar neutrino oscillations 16

1.4.3 Global three-neutrino fits to atmospheric and solar neutrino oscillations 18

1.4.4 Short-baseline neutrino oscillations and the LSND signal . . . 19

1.5 Other experimental searches for neutrino masses and mixings 22

1.6 The MiniBooNE $\nu_\mu \to \nu_e$ search 26

Bibliography 28

Chapter 1

Neutrino oscillations, and the evidence for neutrino masses and mixings

1.1 Neutrinos and the weak interactions: a historical perspective

The history of the neutrino dates back to the very early stages of the Universe, a small fraction of a second after the Big Bang, but it is known to mankind only since 1930. That year, W. Pauli postulated the existence of a neutral particle to explain the continuous energy spectrum of electrons in the β-decay of radioactive nuclei, via (as we know today) $n \rightarrow p + e^- + \bar{\nu}_e$, where $n,\ p,\ e^-,\ \bar{\nu}_e$ indicate a neutron, proton, electron, and electron antineutrino, respectively. After the discovery of the neutron in 1932 by J. Chadwick [1], E. Fermi coins the word "neutrino" to describe this "little, neutral particle", in contrast to the more massive neutron. In 1932, C. D. Anderson discovers the positron [2], the antiparticle of the electron, confirming the prediction of Dirac's relativistic theory of quantum mechanics. In 1934, E. Fermi proposes the first theory of weak interactions [3], successfully describing nuclear β-decay processes. This interaction operates at short, nuclear ranges, and it is termed "weak" in contrast to the nuclear strong interaction inferred by J. Chadwick in 1921, to explain why protons are bound in nuclei despite the electromagnetic, repulsive forces among them. In 1937, E. Majorana first speculates that the hypothetical neutrinos might behave differently than Dirac particles, and that neutrinos and antineutrinos might be indistinguishable [4].

Neutrinos from β-decay were first detected in 1956 by C. Cowan and F. Reines [5], from the decay of neutron-rich nuclei produced in the fission of heavy elements in nuclear reactors. Electron antineutrinos were observed via the detection of the positron emitted in inverse β-decay, $\bar{\nu}_e p \to e^+ n$, and the subsequent γ emission from the neutron capture. The very small interaction rate for this neutrino interaction measured by Cowan and Reines was in rough agreement with Fermi's theory, and confirmed the weak character of neutrino interactions.

After the detection of the neutrino, efforts to try to understand neutrino properties, in particular its mass and spin, started. In 1956, from an analysis of weak particle decays available at the time, Lee and Yang concluded that the weak interactions (unlike the electromagnetic and strong nuclear interactions) do not conserve parity, or equivalently that the formalism describing a process mediated by the weak force is not invariant under a mirror reflection of the physics system under consideration [6]. The year after, C. S. Wu and collaborators unambiguously confirmed parity violation in weak interactions [7].

The non-conservation of parity led Lee and Yang to formulate, in 1957, a "two-component theory" of massless neutrinos [8], in which the half-integer spin neutrinos can only have one possible helicity state, that is only one possible spin orientation with respect to their momentum direction vector, as opposed to the two helicity states allowed for the other particles known in nature. The helicity H of the neutrino was determined to be left-handed in 1958, by Goldhaber *et al.* [9], that is

$H \equiv \vec{p} \cdot \vec{S}/|\vec{p}| = -\hbar/2$, where $\vec{p}$ is the three-momentum vector, $\vec{S}$ the neutrino spin. Parity violation was formally embedded into a new theory of weak interactions, called the (V-A) theory, in that same year, by E. C.G. Sudarshan, R. E. Marshak, and others [12].

During the same period, in 1957, B. Pontecorvo realized that if the neutrino is a massive particle and lepton number is not conserved, then it may oscillate over time or distance into its own antiparticle, the antineutrino [10]. Pontecorvo was not aware of distinct neutrino flavors at the time, and this first oscillation theory was developed in analogy to strangeness oscillations in the neutral kaon system, postulated by Gell-Mann and Pays two years before [11].

Distinct neutrino flavors came as a surprise, when the muon neutrino was discovered in 1962 with the first accelerator-based neutrino beam, by L. Lederman, M. Schwartz, J. Steinberger and collaborators [13]. This neutrino beam technique, consisting in producing a beam of muon neutrinos from pion decays in flight, triggered the exploration of neutrino interactions of significantly higher energies than what was previously achievable. Soon after the discovery of the muon neutrino, Z. Maki, M. Nakagawa and S. Sakata considered the possibility of neutrino oscillations among the electron and the muon flavor states, and introduced neutrino mixing [14].

Another violation of a fundamental physics symmetry in weak interactions, the CP symmetry, was discovered in 1964 by J. W. Cronin and V. Fitch, in the neutral kaon system [15]. The CP operator combines the parity operation P mentioned above, with the charge-conjugation operation C, reversing the sign of charge and magnetic moment of a particle, and therefore implying the interchange of particle and antiparticle. In 1973, M. Koabayashi and T. Maskawa realized that, for CP violation to occur, at least three generations of Dirac particles needed to exist [16]. In 1967, A. D. Sakharov first pointed out that CP violation in weak interactions could be related to the matter-antimatter asymmetry present in the Universe today [17]. While the discovery of CP violation and its possible cosmological connection were derived from the quark sector, it is believed today that they might also be applicable to the neutrino sector.

In the 1960s, the gauge theory of electroweak interactions as we know it today was developed by S. L. Glashow. S. Weinberg and A. Salam [18]. Important aspects of the electroweak theory are the unification of the weak and electromagnetic interactions, the prediction of neutral weak interactions, and the spontaneous symmetry breaking via the Higgs mechanism [20], generating masses for the gauge vector bosons mediating the charged and neutral weak interactions. The neutral current weak interaction of neutrinos, characterized by a neutrino in its final state (and not a charged lepton, as for charged weak interactions), was first detected in 1973 by the Gargamelle bubble chamber experiment at CERN [21]. The massive, charged and neutral, gauge vector bosons postulated by the electroweak theory were first observed by the UA1 experiment at the CERN SPS collider in 1983 [22].

Also during the 1960s, the exploration of the nuclear fusion processes in the core of the Sun via the weakly-interacting neutrinos started. In 1968, R. Davis and collaborators first measured a deficit of solar neutrinos compared to the predictions of the Solar Standard Model, with the Homestake chlorine detector [23]. In the following years, the detection of solar neutrinos was firmly established, but the deficit with respect to expectations remained. Already in 1968, V. N. Gribov and B. Pontecorvo proposed neutrino oscillations among the two types of neutrinos known at the time, the electron and the muon neutrino, as a possible mechanism to explain the solar neutrino deficit [25].

In the mid-1980s, large water Cherenkov detectors were built underground to measure the decay of the proton predicted by grand unified theories. While proton decay has not been observed to date, two major discoveries were made with these detectors, related to the observation of two other extraterrestrial sources of neutrinos. First, in 1987, the Kamiokande (Japan) and IMB (USA) detectors simultaneously observed a burst of neutrinos from the SN1987A supernova explosion in the Large

Magellanic Cloud [26]. Second, in 1988, the Kamiokande experiment measured a deficit in the number of muon neutrinos produced by the interactions of cosmic rays in the Earth's atmosphere [27]. The muon neutrino deficit anomaly was later confirmed and interpreted in terms of muon neutrino to tau neutrino oscillations by the Super-Kamiokande experiment, in 1998 [28]. This third type of neutrino, the tau neutrino, was directly observed only in 2000 by the DONUT experiment at Fermilab [29]. However, its existence was postulated since the discovery in 1975 of its electrically charged counterpart, the tau lepton, by M. Perl and collaborators [30], and indirectly observed in 1989 via precision electroweak measurements at the LEP electron-positron collider at CERN [31].

After the discovery of the solar neutrino deficit by the Homestake chlorine experiment, the exploration of solar neutrinos continued on both the theoretical and experimental fronts. In the late 1970s and early 1980s, S. P. Mikheev, A. Y. Smirnov and L. Wolfenstein formulated neutrino oscillations in the presence of dense matter, predicting large matter effects in solar neutrino oscillations [32]. In the early 1980s and early 1990s, the Kamiokande, SAGE, and GALLEX underground experiments confirmed the solar neutrino deficit [34], by detecting neutrinos mostly originated in different solar nuclear fusion reactions than the ones detected by the Homestake chlorine experiment. In 2001, the Super-Kamiokande and SNO experiments unambiguosuly confirmed that solar neutrino oscillations among the three neutrino flavors occur, and that matter effects are present in solar neutrino oscillations [37].

In the 1990s, the trend in experimental neutrino oscillation physics switched back to the use of man-made neutrino sources, from reactors and particle accelerators. Several neutrino experiments studying oscillations were performed, many with short neutrino propagation pathlengths between the neutrino source and the neutrino detection locations, roughly between 10 m and 1 km. No oscillation signals were seen at short baselines, with the exception of a possible indication for muon antineutrino to electron antineutrino oscillations in the accelerator-based LSND experiment at Los

Alamos [38], first reported in 1996 and still unconfirmed. During the same period, long baseline neutrino experiments detected neutrinos produced hundreds of km away from accelerator and reactor sources. In 2002, the K2K accelerator-based experiment confirmed atmospheric neutrino oscillations [39], and the KamLAND reactor-based experiment confirmed solar neutrino oscillations [40].

This concludes the historical account of major experimental discoveries and ideas in particle physics and astrophysics that are closely related to neutrinos and the weak interactions. Among the scientific advances mentioned above, ten have already been awarded with Nobel Prizes in physics.

1.2 Theory of massless and massive neutrinos

1.2.1 Massless neutrinos and the Standard Model

The Standard Model gauge theory of electroweak interactions describe the interactions of neutrinos in terms of the exchange of $W^{\pm}$, Z^0 intermediate vector bosons. The couplings $W\nu l$ and $Z^0\nu\nu$ describe charged-current and neutral-current interactions, respectively, where l refer to charged leptons. In this theory, neutrinos and antineutrinos are massless, and only left-helicity neutrino states ν_L and right-helicity antineutrino states $\bar{\nu}_R$ exist, that is weak interactions involve only two out of the four components of Dirac fields. The chiral left-handed helicity states are given by $\nu_L \equiv [(1-\gamma^5)/2]\nu$, where $\gamma^5 \equiv i\gamma^0\gamma^1\gamma^2\gamma^3$ and γ^μ are Dirac matrices, and correspond, for massless neutrinos, to the helicity states defined in the previous Section. The experimentally observed (V-A) structure of charged weak interactions, or equivalently the fact that left-handed neutrinos couple only to left-handed charged leptons, is embedded in the charged-current interaction lagrangian with electroweak coupling constant g:

$$\mathcal{L}_{CC} = -\frac{g}{\sqrt{2}} W^-_\rho \overline{l_L} \gamma^\rho \nu_L + \text{h.c.} \tag{1.1}$$

by the $SU(2)_L$ gauge symmetry requirement, where $\overline{l_L} \equiv l_L^\dagger \gamma^0$, and L indicates the weak isospin doublet, $I = 1/2$:

$$L \equiv \begin{pmatrix} \nu \\ l \end{pmatrix} \tag{1.2}$$

where $I_3 = 1/2, -1/2$ for ν and l, respectively, in analogy to the proton-neutron isospin doublet in strong interactions. The right-handed charged lepton l_R forms a weak-isospin singlet, $I = 0$. Similarly, the lagrangian describing neutral current interactions is given by:

$$\mathcal{L}_{NC} = -\frac{g}{2\cos\theta_W} Z_\rho^0 \overline{\nu_L} \gamma^\rho \nu_L + \text{h.c.} \tag{1.3}$$

where θ_W is the Weinberg (weak mixing) angle.

The conservation of electric charge and electric current is embedded in the theory by the invariance of the $\mathcal{L}_{CC} + \mathcal{L}_{NC}$ lagrangian under $U(1)_Y$, where the weak hypercharge Y is related to the electric charge Q and the third component of the weak isospin via $Q = I_3 + Y/2$.

The Standard Model electroweak theory assumes three lepton generations, $\alpha = e, \mu, \tau$. This theory assumes an accidental flavor symmetry, that is not imposed by any gauge invariance principle, that preserve the individual L_e, L_μ, L_τ lepton quantum numbers in all weak interactions, where the lepton quantum numbers are defined as $L_e = 1,\ L_\mu = L_\tau = 0$ for the $(\nu_e, e)_L$ weak doublet, and similarly for the muon and tau doublets. The corresponding antiparticles have opposite lepton numbers. Therefore, neutrino flavor oscillations are not allowed in this theory.

Finally, the gauge invariance of the weak interaction lagrangian is spontaneously broken, and all fermions (with the exception of neutrinos) and W, Z gauge bosons acquire mass, via the Higgs mechanism. In this mechanism, a weak isospin doublet of scalar fields is added to the theory, and charged lepton masses are obtained via Yukawa interaction terms in the lagrangian:

$$\mathcal{L}_{D,l} = f_l(\overline{\nu_L} \phi^+ l_R \nu_L + \overline{l_L} \phi^0 l_R) + \text{h.c.} \tag{1.4}$$

where f_l are dimensionless Yukawa couplings and $\phi^{+,0}$ are the two components of the Higgs weak isospin doublet, with electric charge +1 and zero, respectively. After spontaneous symmetry breaking, $\langle\phi^+\rangle = 0$, $\langle\phi^0\rangle = v/\sqrt{2}$ where $v \simeq 246$ GeV is the vacuum expectation value of the Higgs field, the neutrinos remain massless, while the charged leptons acquire a mass $m_{D,l} = f_l v/\sqrt{2}$. The Yukawa mass term for the lepton l, $-\mathcal{L}_{D,l} = m_{D,l}\overline{l_L}l_R + \text{h.c.}$, is called a Dirac mass term. The same mechanism applies for the generation of quark fermion masses. The Yukawa couplings are free parameters of the theory, and set by the experimentally measured fermion masses m via $f \simeq 5.7 \cdot 10^{-6}(m/1\ \text{MeV})$.

1.2.2 The see-saw mechanism for massive neutrinos

Neutrino mass terms can be added to the Standard Model lagrangian in two ways. The first way is in direct analogy to the Dirac masses of quarks and charged leptons, by adding the two extra components of the Dirac neutrino field, the right-handed neutrino and the left-handed antineutrino fields:

$$-\mathcal{L}_D = m_{sD}\overline{\nu_L}\nu_R + \text{h.c.} \tag{1.5}$$

Majorana mass terms can be constructed from the left-handed neutrino states alone, from right-handed neutrino states only, or from both. For example, for right-handed neutrino states only, the Majorana mass term is:

$$-\mathcal{L}_R = \frac{m_R}{2}\overline{(\nu_R)^c}\nu_R + \text{h.c.} \tag{1.6}$$

where $\nu^c = C\bar{\nu}^T$, C is the charge-conjugation operator, and m_R is a free parameter with dimensions of mass. Majorana mass terms in the lagrangian convert particles into their own antiparticles, and are therefore forbidden for all electrically charged fermions because of charge conservation. Moreover, processes involving Majorana mass terms violate the Standard Model total lepton number $L \equiv L_{e,\mu,\tau}$ by two units, which is not a good quantum number anymore.

Neutrino masses, although not measured yet, are known to be small, of the order of 1 eV or less. The explanation of neutrino masses via Dirac mass terms alone require neutrino Yukawa couplings of the order of 10^{-12} or less. The current theoretical prejudice is that neutrino Yukawa couplings with $f_\nu \ll 1$ and $f_\nu \ll f_l$ are unnatural, if not unlikely.

The so-called see-saw mechanism provides a way to accomodate neutrino masses that is considered more “natural”. The simplest realization of the see-saw model is to add both a Dirac mass term and a right-handed mass term to the lagrangian, as given by Eqs. 1.5 and 1.6, for each of the three neutrino flavors. For each neutrino flavor, two fields of definite chirality and definite mass are obtained. Assuming neutrino Yukawa couplings of the order of the charged fermion couplings, and $m_R \gg v \gtrsim m_D$ of the order of some high mass scale where new physics responsible for neutrino masses is supposed to reside, the see-saw mechanism yields a small light-handed neutrino mass eigenvalue of $m_i \simeq m_D^2/m_R$ and a large right-handed neutrino mass eigenvalue of $m_{3+i} \simeq m_R$, where $i = 1, 2, 3$ runs over the three fermion generations of the Standard Model. The corresponding mass eigenfields ν_i and ν_{3+i} are found to be equal to their corresponding charge-conjugate fields, $\nu_i^c = \nu_i$ and $\nu_{3+i}^c = \nu_{3+i}$. Particles described by fields satisfying this (Majorana) condition are called Majorana particles. Majorana particles and Majorana antiparticles are identical, and are truly neutral particles in the sense that they do not have neither electrical nor any other charges. Neutrinos whose fields do not satisfy this Majorana condition are called Dirac neutrinos. In the Standard Model case of left-handed neutrino fields only, there is no physical difference between massless Majorana neutrinos and massless Dirac neutrinos, while the Dirac/Majorana nature of neutrinos is in principle observable in the case of massive neutrinos.

The neutrino couplings to the W and Z bosons are unaffected by Dirac and/or Majorana mass terms in the lagrangian, and therefore only the left-handed, active, neutrinos participate in weak interactions, while their right-handed partners don’t, and are called sterile neutrinos.

1.3 Neutrino mixing and flavor oscillations

As discussed above, neutrinos only interact via weak processes. Experimentally, this implies that neutrinos are both produced and detected as weak eigenstates. In contrast, the free propagation of neutrinos between their production and detection point is governed by the free hamiltonian, whose eigenstates are states with definite neutrino mass. Nothing requires that neutrino weak and mass eigenstates coincide. In the case in which a weak eigenstate is expressed by a mixture (linear combination) of more than one mass eigenstate, and the neutrino mass eigenvalues in this mixture are different from each other, oscillations among neutrino flavors can be observed as a function of propagation time/distance.

Neutrinos of a given weak flavor $\alpha = e, \mu, \tau$ are defined as the neutrinos produced or detected in association with the charged lepton l_α, in the charged weak interactions described by:

$$-\mathcal{L}_{CC} = \frac{g}{\sqrt{2}} W_\rho^- \sum_{\alpha=e,\mu,\tau} \overline{l_{L\alpha}} \gamma^\rho \nu_{L\alpha} + \text{h.c.} \tag{1.7}$$

In a straightforward generalization of the simplest see-saw mechanism presented above to include three generations, the three weak eigenstates $|\nu_\alpha\rangle$ are generally expressed in terms of a linear combination of six eigenstates $\nu_i(t)$:

$$|\nu_\alpha\rangle = U^*_{\alpha i} |\nu_i\rangle \tag{1.8}$$

where $\alpha = e, \mu, \tau$, $i = 1, \ldots, 6$, and U is a 6×6 unitary mixing matrix diagonalizing the 6×6 symmetric, generally complex neutrino mass matrix M_{D+R} in the weak basis, via the unitary transformation $U^T M_{D+R} U = M_{diag}$, where M_{D+R} is now specified in terms of the 3×3 matrix blocks m_D and m_R:

$$M_{D+R} = \begin{pmatrix} 0 & (m_D)^T \\ m_D & m_R \end{pmatrix} \tag{1.9}$$

From Eq. 1.8 and from the time evolution of free neutrinos, the propagation of a neutrino produced as weak eigenstate α at time t and distance L is:

$$|\nu_\alpha(t)\rangle = \sum_k U^*_{\alpha k} e^{-i(E_k t - p_k L)} |\nu_k\rangle = \sum_{\beta=e,\mu,\tau} (\sum_k U^*_{\alpha k} e^{-i(E_k t - p_k L)} U_{\beta k}) |\nu_\beta\rangle \tag{1.10}$$

Therefore, the probability to detect a neutrino of weak eigenstate β, after a time t from its production as weak eigenstate α, is:

$$P_{\nu_\alpha \to \nu_\beta}(t) = |\langle \nu_\beta | \nu_\alpha(t)\rangle|^2 = |\sum_k U^*_{\alpha k} e^{-i(E_k t - p_k L)} U_{\beta k}|^2 \tag{1.11}$$

If neutrinos are ultrarelativistic, then $t \simeq L$, and furthermore if neutrinos are produced with definite energy E, then $E - p_k \simeq m_k^2/(2E)$. By reabsorbing the phase $e^{-i(E-p_1)L}$, in the ultrarelativisitc regime Eq. 1.11 can be rewritten as:

$$P_{\nu_\alpha \to \nu_\beta}(t) = |\sum_i U^*_{\alpha i} e^{-i\Delta m^2_{i1} L/(2E)} U_{\beta i}|^2 \tag{1.12}$$

where we have defined $\Delta m^2_{i1} \equiv m_i^2 - m_1^2$. By developing the product, using simple trigonometric identities, and reintroducing $\hbar$, c, Eq. 1.13 can be recast into the form [41]:

$$\begin{aligned} P(\nu_\alpha \to \nu_\alpha; L, E) = \delta_{\alpha\beta} - 4 \sum_{j,k} \mathcal{R}(U^*_{\alpha i} U_{\beta i} U_{\alpha j} U^*_{\beta j}) \sin^2[\Delta m^2_{ij} L/(4\hbar c E)] + \\ +2 \sum_{i>j} \mathcal{I}(U^*_{\alpha i} U_{\beta i} U_{\alpha j} U^*_{\beta j}) \sin[\Delta m^2_{ij} L/(2\hbar c E)] \end{aligned} \tag{1.13}$$

where $\mathcal{R}$ and $\mathcal{I}$ indicate the real and imaginary parts, respectively. For antineutrino oscillation probability is obtained from Eq. 1.13, by replacing the mixing matrix U by its complex-conjugate. Therefore, if the mixing matrix is not real, neutrino and antineutrino oscillation probabilities can differ. Furthermore, from Eq. 1.13, it follows directly that neutrino flavor oscillations ($\alpha \neq \beta$) are possible only if neutrino weak and mass eigenstates do not coincide (non-diagonal neutrino mixing matrix U) and neutrino mass eigenvalues are not all degenerate ($\Delta m^2_{ij} \neq 0$ for at least one (i, j) pair). Moreover, Eq. 1.13 shows that neutrino oscillations in vacuum are not sensitive to the sign of the mass splittings Δm^2_{ij}. In very dense matter environments, the neutrino propagation cannot be considered as a free propagation, and matter effects modify Eq. 1.13 in a way that is not symmetric under the change $\Delta m^2_{ij} \rightarrow -\Delta m^2_{ij}$. A special case of neutrino oscillations in matter will be considered in the next Chapter.

If no specific assumptions on the physics mechanisms that generate neutrino masses and mixings are made, how many independent parameters need to be measured, experimentally? Considering N neutrino species, there are N independent neutrino mass parameters. In neutrino oscillation experiments, there are $N-1$ independent mass splittings, for example $\Delta m^2_{i,i-1}$, $i = 2, \ldots, N$. Also, a (generally complex) $N \times N$ mixing matrix contains N^2 independent, real parameters. These can be subdivided into $N(N-1)/2$ mixing angles and $N(N+1)/2$ phases. In the case of Dirac neutrinos, there are $(N-1)(N-2)/2$ physical phases, all of which can be in principle detected in oscillation experiments. In the case of Majorana neutrinos, there are $N-1$ additional physical, Majorana phases. Majorana phases, unlike Dirac phases, cannot be measured in neutrino oscillation experiments, but can be in principle be detected in different experiments (see Section 1.5).

The expression given above, with its 6×6 neutrino mixing matrix, represents the general case for Majorana neutrinos produced via a see-saw model. In this general case, the three sterile neutrino states can be described in terms of the same mixing matrix U (its last three rows) and the same six mass eigenstates as the three active states. Therefore, both oscillations among active netrino flavors and active-sterile neutrino oscillations are in principle observable [42]. Oscillations only among active flavors are observable in two, more commonly considered, cases, and a 3×3 mixing matrix involving only three neutrinos is sufficient. The first case is the one in which sterile neutrinos are very heavy, $m_R > v$ where v is the electroweak energy scale, as typically assumed. In this case, the mixings $U_{\alpha i}$, with $i > 3$, are greatly suppressed, by factors proportional to m_D/m_R. The second case is the one of Dirac neutrinos from a minimally extended Standard Model theory, that is neutrinos whose masses are generated by the addition of a Dirac mass term only in the lagrangian. In this case, sterile neutrinos decouple from the theory, and are not physically observable. We will give some examples of the phenomenology of active-sterile neutrino oscillations in the next Chapter, while below we consider two important special cases: active three-neutrino and active two-neutrino mixings. We focus on neutrino oscillations phenomenology, and we drop Majorana phases from the discussion.

The neutrino pathlengths L and energies E probed in neutrino experiments are such that, often, Eq. 1.13 can be recast in terms of a single mass splitting. This limit is sometimes called the "one mass scale dominance" limit, or the "quasi-two neutrino mass approximation". By making the further assumption that only two neutrino weak eigenstates ($\alpha, \beta = e, \mu$ for definitiveness) and two mass eigenstates ($i = 1, 2$) are relevant, Eq. 1.13 can be written as:

$$\begin{aligned} P(\nu_\alpha \to \nu_\beta) = \delta_{\alpha\beta} - 4\mathcal{R}(U^*_{\alpha 2} U_{\beta 2} U_{\alpha 1} U^*_{\beta 1}) \sin^2[\Delta m^2 L/(4\hbar c E)] + \\ +2\mathcal{I}(U^*_{\alpha 2} U_{\beta 2} U_{\alpha 1} U^*_{\beta 1}) \sin[\Delta m^2 L/(2\hbar c E)] \end{aligned} \tag{1.14}$$

where $\Delta m^2 \equiv \Delta m^2_{21}$. From the discussion above, the physical parameters in the 2×2 mixing matrix are one mixing angle θ and no Dirac phases. The mixing angle θ specifies the rotation among weak eigenstates and mass eigenstates:

$$U = \begin{array}{c c} & \begin{array}{cc} 1 & 2 \end{array} \\ \begin{array}{c} e \\ \mu \end{array} & \left(\begin{array}{cc} \cos\theta & \sin\theta \\ -\sin\theta & \cos\theta \end{array} \right) \end{array} \tag{1.15}$$

Let us assume now that $\alpha = \mu, \beta = e$. From Eqs. 1.14 and 1.15, the two-neutrino oscillation probability formula is:

$$P(\nu_\mu \to \nu_e) = \sin^2 2\theta \sin^2[\Delta m^2 L/(4\hbar c E)] \simeq \sin^2 2\theta \sin^2[1.27 \Delta m^2 (eV^2) L(km)/E(GeV)] \tag{1.16}$$

with $P(\nu_\mu \to \nu_\mu; L, E) = 1 - P(\nu_\mu \to \nu_e; L, E)$.

In the case of three-neutrino mixing, there are two independent mass splittings Δm^2_{21}, Δm^2_{32}, three mixing angles θ_{12}, θ_{13}, θ_{23}, and one Dirac phase δ. A common parametrization for the 3×3 mixing matrix is:

$$
\begin{aligned}
U = & \begin{pmatrix} 1 & 0 & 0 \\ 0 & c_{23} & s_{23} \\ 0 & -s_{23} & c_{23} \end{pmatrix} \begin{pmatrix} c_{13} & 0 & s_{13}e^{-i\delta} \\ 0 & 1 & 0 \\ -s_{13}e^{i\delta} & 0 & c_{13} \end{pmatrix} \begin{pmatrix} c_{12} & s_{12} & 0 \\ -s_{12} & c_{12} & 0 \\ 0 & 0 & 1 \end{pmatrix} = \\
= & \begin{pmatrix} c_{12}c_{13} & s_{12}c_{13} & s_{13}e^{-i\delta} \\ (-s_{12}c_{23} - c_{12}s_{23}s_{13}e^{i\delta}) & (\ c_{12}c_{23} - s_{12}s_{23}s_{13}e^{i\delta}) & s_{23}c_{13} \\ (\ s_{12}s_{23} - c_{12}c_{23}s_{13}e^{i\delta}) & (-c_{12}s_{23} - s_{12}c_{23}s_{13}e^{i\delta}) & c_{23}c_{13} \end{pmatrix}
\end{aligned}
\tag{1.17}
$$

where $c_{ij} \equiv \cos\theta_{ij}$ and $s_{ij} \equiv \sin\theta_{ij}$

1.4 Experimental signatures for neutrino oscillations

Neutrino oscillations are inferred from a discrepancy between the number of observed neutrino interactions with respect to the number of interactions predicted assuming no oscillations. Moreover, since the oscillation probability is in general affected by the neutrino energy, the extent of this discrepancy is neutrino energy-dependent. Two types of oscillation measurements are possible. The first type is an "appearance" measurement, where a neutrino of some weak flavor type is produced (say, a muon neutrino), and a different neutrino type (e.g., an electron neutrino) is observed at some distance from the neutrino source. The second type is a "disappearance" measurement, where a known amount of neutrinos of some weak flavour type is produced, and a smaller amount of that same weak flavour type is observed after some distance/time.

If a discrepancy between observations and predictions assuming no oscillations is present, one can then find what are the possible oscillation hypotheses that are compatible with the observations, if any.

1.4.1 Atmospheric neutrino oscillations

The disappearance of muon neutrinos produced by cosmic ray interactions in the atmosphere has now been firmly established using large undeground water Cherenkov detectors. Atmospheric neutrinos that can be cleanly reconstructed in these detectors are typically produced with an energy $E \sim 1-10$ GeV, and travel distances $L \sim 10^2 - 10^4$ km, where the shortest distance corresponds to downward-going neutrinos produced in the atmosphere above the detector, and the longest distance corresponds to upward-going neutrinos produced in the atmosphere at the antipodes and crossing the Earth's diameter, before interacting in the detector. Therefore, these experiments cover the wide range $L/E \sim 1-10^4$ km/GeV, and neutrino oscillations in the range $\Delta m^2 \sim 10^{-4} - 1\ eV^2$ may cause observable L/E spectral distortions. The current-generation, atmospheric water Cherenkov detector is the Super-Kamiokande detector in Japan. The neutrino energy and direction is estimated from the total momentum vector magnitude and direction of final state particles from the neutrino interaction, reconstructed via the Cherenkov ring pattern. The pattern of the most energetic Cherenkov ring is used to distinguish electron neutrino from muon neutrino interactions. The number of observed downward-going muon neutrinos (small L/E) is consistent with the number expected for no neutrino oscillations, while only about half of upward-going muon neutrino interactions are observed, compared to the no-oscillation hypothesis. Moreover, the number of electron neutrinos observed at all L/E is consistent with the Standard Model expectation. Overall, the Super-Kamioande data can be explained via $\nu_\mu \to \nu_\tau$ oscillations due to full mixing ($\theta \simeq \pi/4$) and $\Delta m^2 \simeq 2.4 \cdot 10^{-3}\ eV^2$. More stringent limits on $\nu_\mu \to \nu_e$ oscillations at this Δm^2 scale have been obtained by the CHOOZ reactor antineutrino experiment, which did not measure any disappearance of few MeV electron antineutrinos over pathlengths of $L \sim 1$ km. The ratio of observed-to-predicted L/E distributions for muon neutrino interactions at Super-Kamiokande is given in the left panel of Fig. 1.1, together with the best-fit $\nu_\mu \to \nu_\tau$ hypothesis, and two alternative, beyond the Standard Model

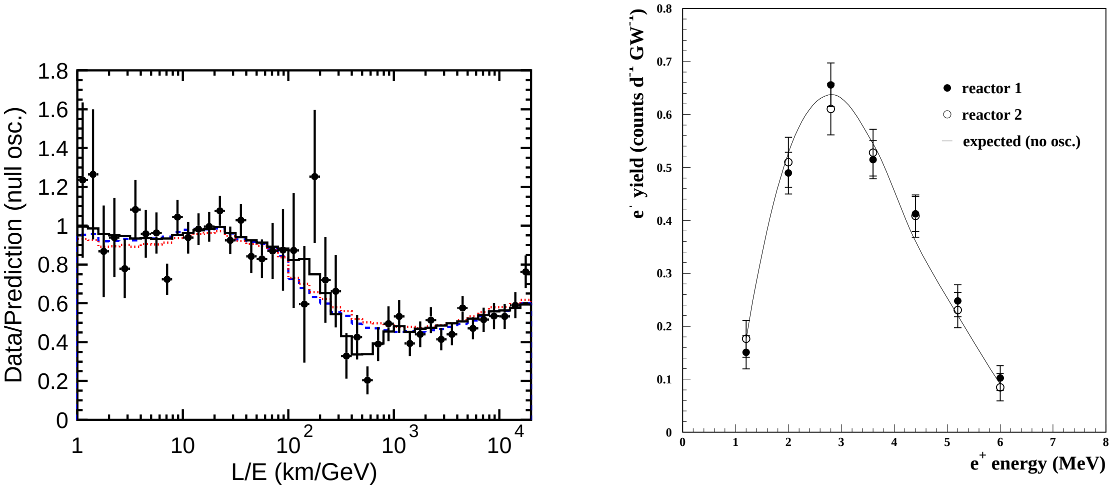

Figure 1.1: *Left: points indicate the ratio of observed to predicted (for no oscillations) muon neutrino events at Super-Kamiokande, as a function of the reconstructed* L/E*, together with the best-fit hypotheses for* $\nu_\mu \to \nu_\tau$ *oscillations (solid line), neutrino decay (dashed), and neutrino decoherence (dotted) [43]. Right: points indicate the positron yields from* $\bar{\nu}ep \to e^+n$ *interactions, as a function of positron energy, observed by the CHOOZ experiment; the solid line show the yield expected for no-oscillations [44].*

explanations of neutrino data, neutrino decay and neutrino decoherence, which are disfavored compared to oscillations [43]. The observed energy distribution of positron events from $\bar{\nu}_e p \to e^+ n$ interactions at CHOOZ is given in the right panel of Fig. 1.1, together with the no-oscillation prediction [44]. The Super-Kamiokande atmospheric result has recently been confirmed by the K2K experiment [39], which uses the same Super-Kamiokande detector, and ~ 1 GeV muon neutrinos from a accelerator-based source located 250 km away from the detector.

1.4.2 Solar neutrino oscillations

The most convincing evidence to date that solar electron neutrinos oscillate into other active neutrino flavors (ν_μ or ν_τ) comes from the SNO experiment in Canada. The

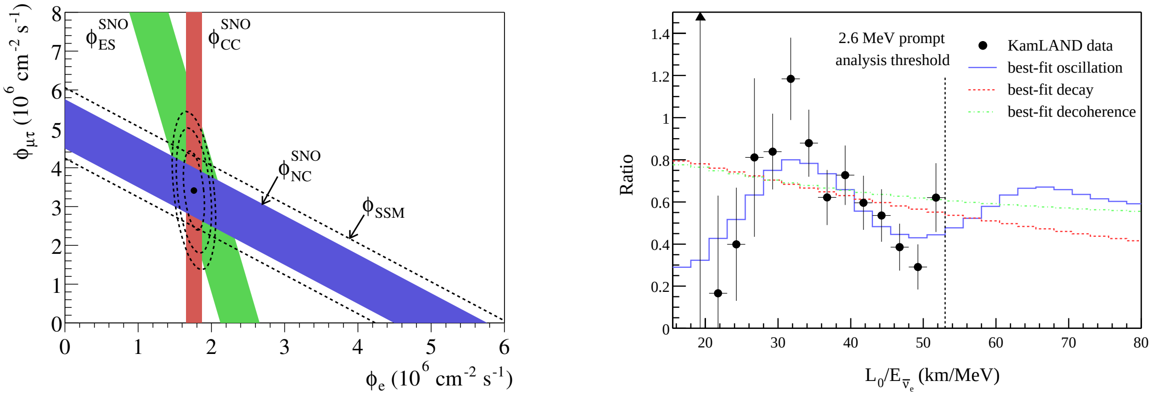

Figure 1.2: *Left: solar muon or tau neutrino flux versus electron neutrino flux, as measured by three different neutrino reactions with the SNO detector [45]; the dashed lines enclose the Solar Standard Model prediction [46]. Right: points indicate the* $\bar{\nu}_e$ *spectrum observed in KamLAND, divided by the no-oscillation expectation, as a function of* L_0/E*. The curves indicate the best-fit neutrino oscillation, decay, and decoherence hypotheses [47].*

SNO detector is also an underground Cherenkov detector, filled with heavy water (D_2O), capable of detecting few MeV solar neutrino interactions via the charged-current (CC) process $\nu_e d \rightarrow ppe^-$, the neutral-current (NC) process $\nu_\alpha d \rightarrow pn\nu_\alpha$, and the elastic scattering (ES) process $\nu_\alpha e^- \rightarrow \nu_\alpha e^-$. While the CC process is only sensitive to electron neutrinos, the NC and ES processes are sensitive to all active neutrino flavors ν_α, $\alpha = e, \mu, \tau$. The left panel in Figure 1.2 shows the solar neutrino fluxes $\phi_{\mu,\tau}$ and ϕ_e estimated by the SNO measurements [45]. The total active neutrino flux $\phi_{\mu,\tau} + \phi_e$ is in good agreement with the Solar Standard Model expectation ϕ_{SSM} [46]. On the other hand, only about a third of the originally produced electron neutrinos is detected on Earth.

In general, results from different solar neutrino experiments are affected by neutrino oscillations in a different way, depending on their energy threshold for neutrino detection. By combining the SNO results with the results from the Super-Kamiokande, Homestake, and gallium experiments, and by taking into account matter effects inside the Sun and Earth, it is found that solar neutrino oscillations are consistent with $\nu_e \rightarrow \nu_{\mu,\tau}$ oscillations specified by a mixing angle θ with $\tan^2\theta \simeq 0.4$, and $\Delta m^2 \simeq 8 \cdot 10^{-5}\ eV^2$. For this Δm^2 range, matter effects play a dominant role on neutrino oscillations, allowing to resolve the $(\theta \leftrightarrow \pi/2 - \theta)$ degeneracy of vacuum neutrino oscillations.

The KamLAND experiment in Japan has confirmed solar neutrino oscillations by detecting the disappearance of few MeV electron antineutrinos produced at nuclear reactors located a few hundreds of km away from the liquid scintillator KamLAND detector [40]. Electron antineutrino interactions $\bar{\nu}_e p \rightarrow n e^+$ are tagged by the prompt positron signal, and the 2.2 MeV γ ray from the $\sim 200\ \mu s$ delayed neutron capture signal. The positron energy is used to estimate the $\bar{\nu}_e$ energy E event-by-event, while the average neutrino pathlength $L_0 \simeq 180$ km is inferred from simulations. The L_0/E distirbution of KamLAND data is shown in the right panel of Fig. 1.2, together with the best-fit neutrino oscillation, neutrino decay, and neutrino decoherence hypotheses [47]. As for atmsopheric neutrinos, the disappearance of reactor antineutrinos is well explained by neutrino oscillations, while mechanisms other than oscillations are highly disfavored.

1.4.3 Global three-neutrino fits to atmospheric and solar neutrino oscillations

Solar and atmospheric neutrino oscillation data can be collectively analyzed. It is found [48] that all these datasets are consistent with oscillations among the three neutrino flavors ν_e, ν_μ, ν_τ. Furthermore, the mass splittings Δm^2_{21}, Δm^2_{32}, and the mixing angles θ_{12}, θ_{23}, θ_{13} appearing in Eq. 1.17, describing three-neutrino oscillations are now relatively well kwown, as shown by the results of a global fit given in Fig. 1.3 [48]. Present data also measure the sign of the solar mass splitting Δm^2_{21} (or equivalently the θ_{12} octant). On the other hand, the sign of the atmospheric mass splitting Δm^2_{32} and the value of the Dirac CP-violating phase δ are currently unknown. Experiments are now being planned to probe these two parameters, as well as to

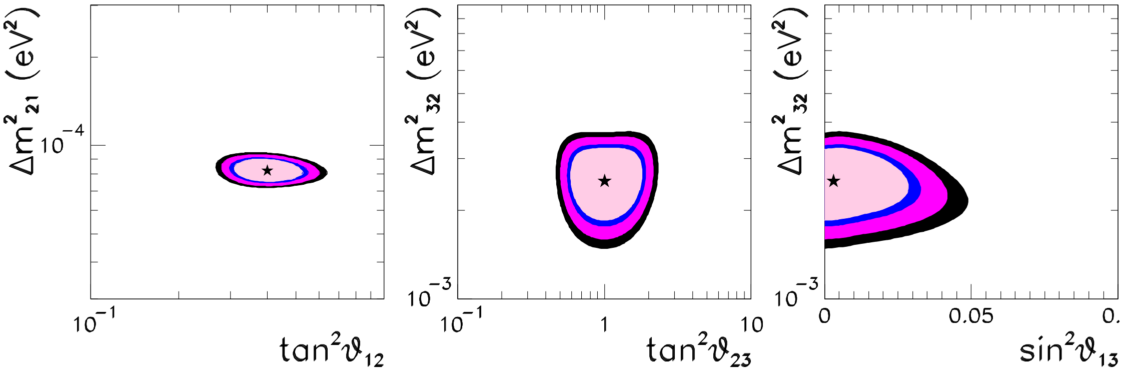

Figure 1.3: *Allowed ranges for the three-neutrino mass and mixing parameters* Δm^2_{21}, Δm^2_{31}, θ_{12}, θ_{23}, *and* θ_{13}, *from global fits of solar and atmospheric oscillation data [48]. The regions correspond to 90%, 95%, 99% and 3* σ *confidence level.*

extend the θ_{13} sensitivity.

1.4.4 Short-baseline neutrino oscillations and the LSND signal

Several neutrino oscillation searches have been performed to probe higher Δm^2 values than what indicated by solar and atmospheric neutrino oscillations. In these searches, the possible appearance or disappearance of neutrinos produced at accelerators and reactors over distances $L \sim 10^{-2} - 1$ km is studied, and these experiments are generally called short-baseline experiments. Several oscillation channels have been explored, as summarized in Tab. 1.1.

The only positive oscillation result among the short-baseline oscillation searches is the evidence for $\bar{\nu}_\mu \to \bar{\nu}_e$ oscillations reported by the Liquid Scintillator Neutrino Detector (LSND) experiment at Los Alamos Laboratories (USA) [38]. A muon antineutrino source with a known energy distribution with enpoint of 52.8 MeV is produced via the π^+/μ^+ decay at rest chain $\pi^+ \to \mu^+\nu_\mu$, $\mu^+ \to e^+\nu_e\bar{\nu}_\mu$, with little $\bar{\nu}_e$ contamination. At detection, about 30 m away from the neutrino source, a $\bar{\nu}_e$ excess

Channel	Experiment	Optimal Δm^2	Low Δm^2 Reach	$\sin^2 2\theta$ Constraint		Ref.
				High Δm^2	Optimal Δm^2	
$\nu_\mu \to \nu_e$	LSND	$2 \cdot 10^0$	$3 \cdot 10^{-2}$	$[2.5 - 3.8] \cdot 10^{-3}$	$[1.2 - 3.2] \cdot 10^{-3}$	[38]
	KARMEN	$3 \cdot 10^0$	$6 \cdot 10^{-2}$	$< 1.7 \cdot 10^{-3}$	$< 1.0 \cdot 10^{-3}$	[49]
	NOMAD	$3 \cdot 10^1$	$4 \cdot 10^{-1}$	$< 1.4 \cdot 10^{-3}$	$< 1.0 \cdot 10^{-3}$	[50]
$\nu_e \to \nu_{\not e}$	Bugey	$6 \cdot 10^{-1}$	$1 \cdot 10^{-2}$	$< 1.4 \cdot 10^{-1}$	$< 1.3 \cdot 10^{-2}$	[51]
	CHOOZ	$6 \cdot 10^{-3}$	$7 \cdot 10^{-4}$	$< 1.0 \cdot 10^{-1}$	$< 5 \cdot 10^{-2}$	[44]
$\nu_\mu \to \nu_{\not \mu}$	CCFR84	$9 \cdot 10^2$	$6 \cdot 10^0$	none	$< 2 \cdot 10^{-1}$	[52]
	CDHS	$3 \cdot 10^0$	$3 \cdot 10^{-1}$	none	$< 5.3 \cdot 10^{-1}$	[53]
$\nu_\mu \to \nu_\tau$	NOMAD	$1 \cdot 10^2$	$7 \cdot 10^{-1}$	$< 3.3 \cdot 10^{-4}$	$< 2.5 \cdot 10^{-4}$	[54]
	CHORUS	$6 \cdot 10^1$	$5 \cdot 10^{-1}$	$< 6.8 \cdot 10^{-4}$	$< 4.5 \cdot 10^{-4}$	[55]
$\nu_e \to \nu_\tau$	NOMAD	$1 \cdot 10^2$	$6 \cdot 10^0$	$< 1.5 \cdot 10^{-2}$	$< 1.1 \cdot 10^{-2}$	[54]
	CHORUS	$9 \cdot 10^1$	$7 \cdot 10^0$	$< 5.1 \cdot 10^{-2}$	$< 4 \cdot 10^{-2}$	[55]

Table 1.1: *Most sensitive short- and medium-baseline neutrino oscillation searches in various oscillation channels.* Δm^2 *is expressed in* eV^2*, and the low* Δm^2 *reach and* $\sin^2 2\theta$ *constraints are given at the 90% confidence level.*

is seen by tagging the positron and the γ from neutron capture from the inverse β decay reaction, $\bar{\nu}_e p \to e^+ n$. The neutrino energy E_ν is estimated from the measured positron energy and emission angle, using two-body kinematics. The excess has a 3.8σ significance, and its L/E_ν dependence is compatible with oscillations, as shown in the left panel of Fig. 1.4. The KARMEN experiment at the Rutherford Laboratory (UK) performed a $\bar{\nu}_\mu \to \bar{\nu}_e$ search with a neutrino source and detection principle that are similar to the LSND ones [49]. The main differences between the two experiments' oscillation sensitivities are due to the shorter KARMEN baseline of $L = 17.7$ m, and the weaker KARMEN statistical power. The KARMEN results are compatible with no $\bar{\nu}_\mu \to \bar{\nu}_e$ oscillations, and are shown in the right panel of Fig. 1.4 as a function of positron, prompt energy.

The LSND-allowed and KARMEN-excluded regions in two-neutrino oscillation

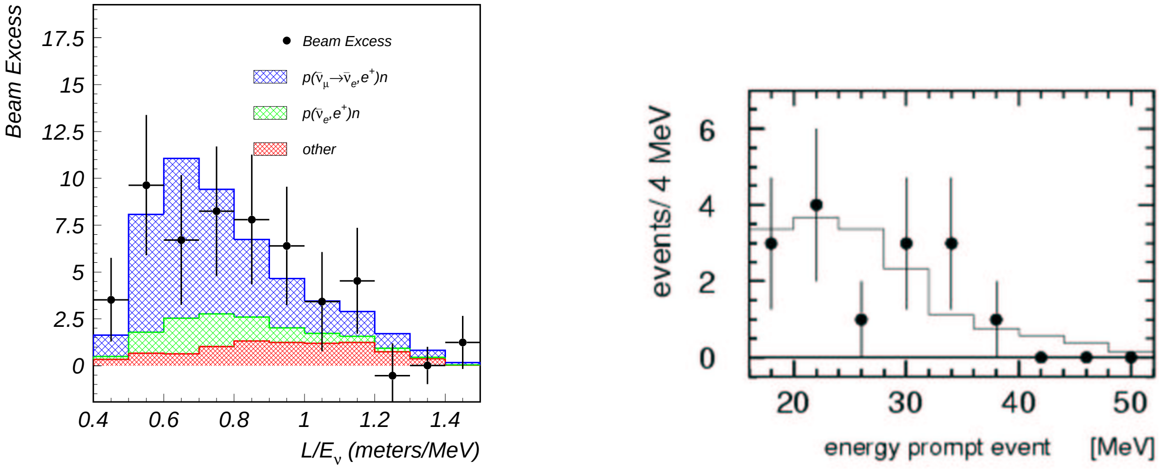

Figure 1.4: *Left: the points show the L/E distribution of* $\bar{\nu}_e$ *candidate events observed in LSND; the red and green histograms show the expectations for no oscillations, and the blue histogram show the best-fit oscillation contribution. Right: the points indicate the prompt, visible energy distribution observed in KARMEN, and the histogram shows the expectation for no oscillations.*

parameter space $(\sin^2 2\theta, \Delta m^2)$ are shown in the left panel of Fig. 1.5, together with the exclusion region from a null electron antineutrino disappearance search with the Bugey experiment [38, 49, 51]. The KARMEN and Bugey null oscillation results exclude a part of the LSND allowed region, while another part has not yet been refuted nor confirmed by any neutrino experiment other than LSND. A joint LSND-KARMEN oscillation analysis has been performed by collaborators from both experiments [56]. The analysis yields a level of 64% compatibility of the two experimental outcomes. Assuming statistical compatibility, the joint allowed region in oscillation parameters space, shown in the right panel of Fig. 1.5, is consistent with the LSND-only region.

The LSND oscillation evidence at high Δm^2, in conjunction with the solar and atmospheric neutrino oscillation results, cannot be accomodated within the simplest Standard Model extension possible, that is one with only three, active, massive neutrinos. In simple terms, the reason stems from the fact that $\Delta m^2_{LSND} \gg$

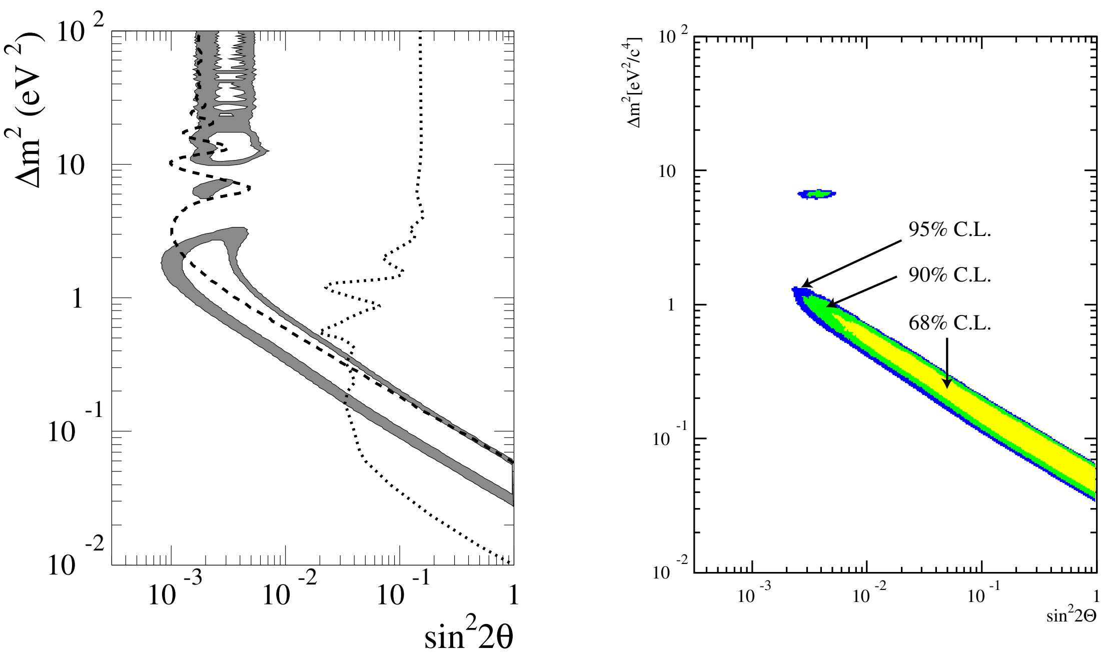

Figure 1.5: *Left: the filled area shows the LSND 90% and 99% CL allowed region in oscillation parameter space [38]; the dashed and dotted curves show the 90% CL upper limits on* $\bar{\nu}_\mu \to \bar{\nu}_e$ *oscillations from KARMEN [49], and* $\bar{\nu}_e \to \bar{\nu}_{\not e}$ *oscillations from Bugey [51]. Right: joint LSND-KARMEN allowed region in oscillation parameter space, assuming statistical compatibility among the two experimental outcomes [56].*

$\Delta m^2_{atm} + \Delta m^2_{sol}$, in contrast with the expectation from three-neutrino oscillation models, that is $\Delta m^2_{31} \equiv \Delta m^2_{32} + \Delta m^2_{21}$.

1.5 Other experimental searches for neutrino masses and mixings

Neutrino oscillations experiments are not the only way to probe neutrino masses and mixings. We briefly discuss here three more examples: tritium β decay kinematics measurements, neutrinoless double β decay searches, and observational cosmology.

Neutrino oscillation experiments cannot measure the absolute scale of neutrino masses. On the other hand, the differential electron energy spectrum in β decay experiments is affected by both neutrino masses, and by the mixings defining the electron neutrino state in terms of mass eigenstates. The region of interest to the study of neutrino properties is located near the β endpoint. The most sensitive searches conducted so far are based upon the decay of tritium, via $^3\mathrm{H} \rightarrow ^3\mathrm{He}^+ e^- \bar{\nu}_e$, mostly because of its very low β endpoint energy of 18.6 keV. For a spectrometer integrating over the electron energy interval δ near the β-decay endpoint, the count rate is [57]:

$$n(\delta) = \frac{\bar{R}}{3} \sum_{i=1}^{n} |U_{ei}|^2 (\delta^2 - m_i^2)^{3/2} \tag{1.18}$$

where the quantity $\bar{R}$ does not depend on the small neutrino masses and mixings, and and only the neutrino masses m_i such that $\delta > m_i$ are considered in the summation. From the experimental point of view, tritium β decay results are generally expressed in terms of a single effective mass $m(\nu_e)$:

$$n_s(\delta) = \frac{\bar{R}}{3} (\delta^2 - m(\nu_e)^2)^{3/2} \tag{1.19}$$

where $m(\nu_e)$ is the fit mass parameter. In the limit $\delta^2 \gg m_i^2$, the relation between the true masses and mixings to the fitted mass $m(\nu_e)$ is independent from the integration interval δ:

$$m(\nu_e)^2 \simeq \sum_{i=1}^{n} |U_{ei}|^2 m_i^2 \tag{1.20}$$

The current best measurements on $m(\nu_e)^2$ come from the Troitsk and Mainz experiments [58], which have very similar $m(\nu_e)^2$ sensitivities. Both found no evidence for a nonzero $m(\nu_e)^2$ value; the latest Mainz result is $m(\nu_e)^2 = -1.6 \pm 2.5 \pm 2.1$ eV^2, or $m(\nu_e) \leq 2.2$ eV at 95% CL, using $\delta = 70$ eV [58]. The planned tritium β decay experiment KATRIN should be able to improve the sensitivity to $m(\nu_e)$ by roughly an order of magnitude in the forthcoming years, thanks to its better statistics, energy resolution, and background rejection [59].

Neutrino oscillations do not probe the neutrino Dirac/Majorana character. On the other hand, the neutrinoless double-beta ($0\nu\beta\beta$) decay process is possible only if neutrinos are Majorana particles, while it is forbidden for Dirac neutrinos. Moreover, assuming that neutrinos are Majorana particles, $0\nu\beta\beta$ searches probe also neutrino masses and mixings. Double-beta decay is a rare nuclear transition accompanied by the simultaneous emission of two electrons. The dominant mode is the second order weak process $(A, Z) \rightarrow (A, Z+2)e^-e^-\bar{\nu}_e\bar{\nu}_e$, or $2\nu\beta\beta$, which conserves lepton number and is therefore allowed within the Standard Model. Neutrinoless double-beta decay proceeds without antineutrino emission, via $(A, Z) \rightarrow (A, Z+2)e^-e^-$. The experimental signature of $0\nu\beta\beta$ is given by a measurement for the sum of the two electron energies consistent with the Q-value of the transition. The $0\nu\beta\beta$ rate $(T^{0\nu}_{1/2})^{-1}$ is related to the effective neutrino Majorana mass $m_{\beta\beta}$ via [60]:

$$(T^{0\nu}_{1/2})^{-1} = G^{0\nu}|M^{0\nu}|^2 m^2_{\beta\beta} \tag{1.21}$$

where $G^{0\nu}$ is a phase space factor, $M^{0\nu}$ is a nuclear matrix element, and the effective Majorana mass is given by:

$$m_{\beta\beta} = |\sum_i U^2_{ei} m_i| \tag{1.22}$$

where the U_{ei} mixing matrix elements are in general complex, and the resulting expression for $m_{\beta\beta}$ may in general depend on both Dirac and Majorana phases. No convincing indication of $0\nu\beta\beta$ has been found, so far, and an upper limit $m_{\beta\beta} \gtrsim 1\ eV$ have been obtained [60]. The uncertainties in the nuclear matrix elements evaluation contribute to about a factor of 3 uncertainty in the Majorana mass uncertainty, for a given $0\nu\beta\beta$ rate. Future experiments with significantly improved sensitivites are being planned.

Observational cosmology can also constrain neutrino properties. Two examples are discussed here: the neutrino energy density during the Big Bang Nucleosynthesis (BBN) era affects the primordial abundances of Helium and other elements, and neutrino masses affect the large scale structure formation of the Universe.

The Helium primordial abundance is set by the neutron-to-proton ratio at weak freeze-out, that is at the epoch (temperature) at which the rate for the weak interaction process $pe^- \leftrightarrow n\nu_e$ equals the expansion rate of the Universe. In general, the higher the neutrino energy density, or equivalently the so-called number of effective neutrino species N_{eff} present during BBN, the higher the expansion rate is, the higher the freeze-out temperature T_f. In the absence of a lepton asymmetry, generally expressed in terms of non-zero neutrino chemical potentials, the neutron-to-proton ratio is related to T_{fo} via $n/p \simeq \exp[-(m_n - m_p)/T]$, where m_n and m_p are the neutron and proton masses, respectively. Therefore, the higher N_{eff}, the higher the neutron-to-proton ratio, and the higher the primordial Helium abundance is. The measured primordial Helium abundance, in conjunction with standard cosmology assumptions, yields $1.7 < N_{eff} < 3.5$ at 95% confidence level [61].

Neutrinos decouple from the the Universe thermal bath when they are relativistic. In this case, the free-streaming scale of neutrinos is therefore of the order of the Universe horizon at that epoch. Over distances smaller than the neutrino free streaming scale, massive neutrinos tend to wash out matter clustering due to gravity. As the Universe expands, massive neutrinos become eventually non-relativistic, their free-streaming scale does not scale as the event horizon anymore, and the effect of neutrinos on structure formation becomes negligible. The observations of the cosmic ray background anysotropies, and of the power spectrum of large-scale matter structure, are consistent with a negligible effect attributed to nonzero neutrino masses, and typical upper limits on the sum of neutrino masses of $\sum_i m_i \lesssim 1\ eV$ are obtained [62].

In particular, cosmology may provide constraints on sterile neutrinos. Predictions of standard cosmology assume that sterile neutrino species are present in the early Universe in the same abundances as the active species. In this picture, massive sterile neutrinos with significant mixing to active neutrinos are expected to alter both the Helium abundance and the matter power spectrum predictions, in disagreement with observations. However, several mechanisms have been proposed that would suppress the sterile neutrino abundances in cosmology: primordial lepton asymmetries [63], low reheating temperature [64], or other, more exotic, possibilities [61].

1.6 The MiniBooNE $\nu_\mu \rightarrow \nu_e$ search

The main goal of the MiniBooNE experiment is to unambiguously confirm or refute the evidence for $\bar{\nu}_\mu \rightarrow \bar{\nu}_e$ oscillations seen by the LSND experiment at Los Alamos. This is important because, as stated above, the LSND oscillation result is incompatible with the robust evidence for solar and atmospheric neutrino oscillations in the simplest three-neutrino mixing paradigm.

The MiniBooNE experiment is probing the oscillation parameter space indicated by LSND via a $\nu_\mu \rightarrow \nu_e$ search, and possibly by a future $\bar{\nu}_\mu \rightarrow \bar{\nu}_e$ search. The large sample of neutrino interactions detected at MiniBooNE will allow to cover the full LSND allowed region at 4σ significance, as shown in the left panel of Fig. 1.6 [65]. Furthermore, the sources of systematic uncertainties affecting the MiniBooNE $\nu_\mu \rightarrow \nu_e$ search are very different than the ones possibly affecting the LSND result. This is because, despite the similar neutrino L/E range measured in the two experiments, neutrinos detected at MiniBooNE are about a factor of 20 more energetic than LSND neutrinos, with typical energies of the order of 1 GeV. In the case of a confirmation of the LSND signal, MiniBooNE will also be able to discern at some level the mass and mixing parameters responsible for neutrino oscillations, as shown in the right panel of Fig. 1.6 [65]. A rough determination of the LSND neutrino mass and mixing parameters would not only be of extraordinary interest in itself, but would also serve as guidance for the planning of future short-baseline experiments such as a two-detector experiment at Fermilab, BooNE.

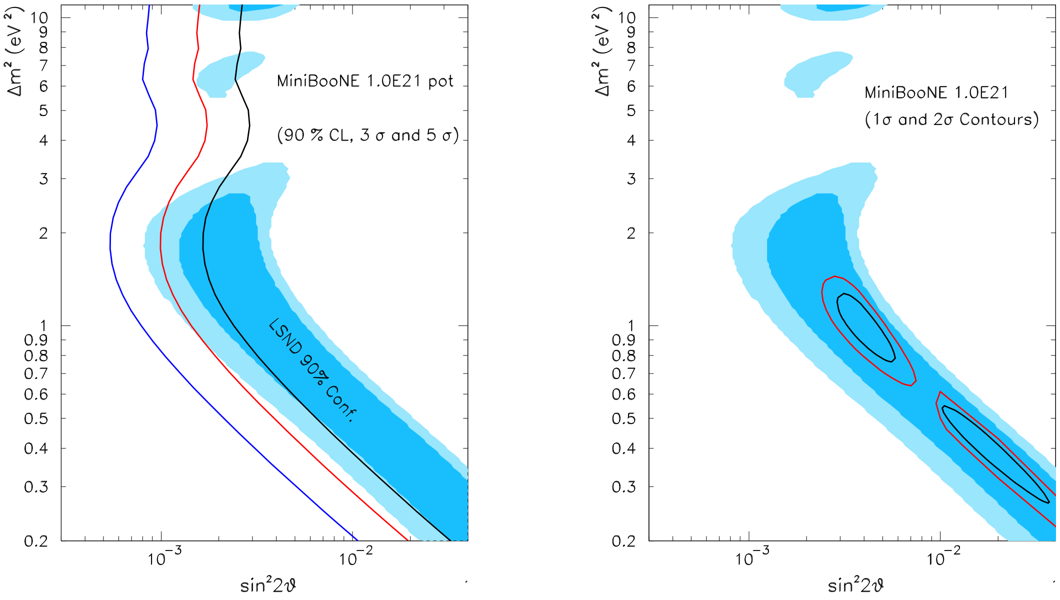

Figure 1.6: *Left: MiniBooNE oscillation sensitivity for* 10^{21} *protons on target. The dark (light) blue areas are the LSND 90% (99%) CL allowed regions. The three curves give the 90%, 3* σ*, and 5* σ *sensitivity regions for MiniBooNE. Right: one and two* σ *contours for an oscillation signal with* $\Delta m^2 = 0.4$ *or* 1.0 eV^2*, and for a data sample corresponding to* 10^{21} *protons on target [65].*

Bibliography

[1] J. Chadwick, *Proc. R. Soc. London (A)* **136**, 692 (1932).

[2] C. D. Anderson, Phys. Rev. **43**, 491 (1933).

[3] E. Fermi, Z. Phys. **88**, 161 (1934).

[4] E. Majorana, Nuovo Cim. **14**, 171 (1937).

[5] C. L. Cowan, F. Reines, F. B. Harrison, H. W. Kruse and A. D. McGuire, Science **124**, 103 (1956).

[6] T. D. Lee and C. N. Yang, Phys. Rev. **104**, 254 (1956).

[7] C. S. Wu, E. Ambler, R. W. Hayward, D. D. Hoppes and R. P. Hudson, Phys. Rev. **105**, 1413 (1957).

[8] T. D. Lee and C. N. Yang, Phys. Rev. **105**, 1671 (1957).

[9] M. Goldhaber, L. Grodzins and A. W. Sunyar, Phys. Rev. **109**, 1015 (1958).

[10] B. Pontecorvo, Sov. Phys. JETP **6**, 429 (1957) [Zh. Eksp. Teor. Fiz. **33**, 549 (1957)].

[11] M. Gell-Mann and A. Pais, Phys. Rev. **97**, 1387 (1955).

[12] E. C. G. Sudarshan and R. e. Marshak, Phys. Rev. **109**, 1860 (1958);
R. P. Feynman and M. Gell-Mann, Phys. Rev. **109**, 193 (1958).

[13] G. Danby, J. M. Gaillard, K. Goulianos, L. M. Lederman, N. Mistry, M. Schwartz and J. Steinberger, Phys. Rev. Lett. **9**, 36 (1962).

[14] Z. Maki, M. Nakagawa and S. Sakata, Prog. Theor. Phys. **28**, 870 (1962).

[15] J. H. Christenson, J. W. Cronin, V. L. Fitch and R. Turlay, Phys. Rev. Lett. **13**, 138 (1964).

[16] M. Kobayashi and T. Maskawa, Prog. Theor. Phys. **49**, 652 (1973).

[17] A. D. Sakharov, Pisma Zh. Eksp. Teor. Fiz. **5**, 32 (1967) [JETP Lett. **5**, 24 (1967 SOPUA,34,392-393.1991 UFNAA,161,61-64.1991)].

[18]

[19] S. L. Glashow, Nucl. Phys. **22**, 579 (1961); S. Weinberg, Phys. Rev. Lett. **19**, 1264 (1967); A. Salam, “Weak And Electromagnetic Interactions,” in *Elementary Particle Theory, Proc. 8th Nobel Symp.*, 367 (1968).

[20] F. Englert and R. Brout, Phys. Rev. Lett. **13**, 321 (1964); P. W. Higgs, Phys. Rev. Lett. **13**, 508 (1964); G. S. Guralnik, C. R. Hagen and T. W. B. Kibble, Phys. Rev. Lett. **13**, 585 (1964); Y. Nambu and G. Jona-Lasinio, Phys. Rev. **122**, 345 (1961); J. Goldstone, Nuovo Cim. **19**, 154 (1961).

[21] F. J. Hasert *et al.* [Gargamelle Neutrino Collaboration], Phys. Lett. B **46**, 138 (1973).

[22] G. Arnison *et al.* [UA1 Collaboration], Phys. Lett. B **122**, 103 (1983); G. Arnison *et al.* [UA1 Collaboration], Phys. Lett. B **126**, 398 (1983).

[23] R. J. Davis, D. S. Harmer and K. C. Hoffman, Phys. Rev. Lett. **20**, 1205 (1968);

[24] B. T. Cleveland *et al.*, Astrophys. J. **496**, 505 (1998).

[25] V. N. Gribov and B. Pontecorvo, Phys. Lett. B **28**, 493 (1969).

[26] K. Hirata *et al.* [KAMIOKANDE-II Collaboration], Phys. Rev. Lett. **58**, 1490 (1987); R. M. Bionta *et al.*, Phys. Rev. Lett. **58**, 1494 (1987).

[27] K. S. Hirata *et al.* [KAMIOKANDE-II Collaboration], Phys. Lett. B **205**, 416 (1988).

[28] Y. Fukuda *et al.* [Super-Kamiokande Collaboration], Phys. Rev. Lett. **81**, 1562 (1998) [arXiv:hep-ex/9807003].

[29] K. Kodama *et al.* [DONUT Collaboration], Phys. Lett. B **504**, 218 (2001) [arXiv:hep-ex/0012035].

[30] M. L. Perl *et al.*, Phys. Rev. Lett. **35**, 1489 (1975).

[31] D. Decamp *et al.* [ALEPH Collaboration], Phys. Lett. B **231**, 519 (1989).

[32] S. P. Mikheev and A. Y. Smirnov, Sov. J. Nucl. Phys. **42**, 913 (1985) [Yad. Fiz. **42**, 1441 (1985)];

[33] L. Wolfenstein, Phys. Rev. D **20**, 2634 (1979).

[34] K. S. Hirata *et al.* [KAMIOKANDE-II Collaboration], Phys. Rev. Lett. **63**, 16 (1989);

[35] A. I. Abazov *et al.*, Phys. Rev. Lett. **67**, 3332 (1991);

[36] P. Anselmann *et al.* [GALLEX Collaboration], Phys. Lett. B **285**, 376 (1992).

[37] S. Fukuda *et al.* [Super-Kamiokande Collaboration], Phys. Rev. Lett. **86**, 5651 (2001) [arXiv:hep-ex/0103032]; Q. R. Ahmad *et al.* [SNO Collaboration], Phys. Rev. Lett. **87**, 071301 (2001) [arXiv:nucl-ex/0106015].

[38] C. Athanassopoulos *et al.* [LSND Collaboration], Phys. Rev. Lett. **77**, 3082 (1996) [arXiv:nucl-ex/9605003]; A. Aguilar *et al.* [LSND Collaboration], Phys. Rev. D **64**, 112007 (2001) [arXiv:hep-ex/0104049].

[39] M. H. Ahn *et al.* [K2K Collaboration], Phys. Rev. Lett. **90**, 041801 (2003) [arXiv:hep-ex/0212007].

[40] K. Eguchi *et al.* [KamLAND Collaboration], Phys. Rev. Lett. **90**, 021802 (2003) [arXiv:hep-ex/0212021].

[41] B. Kayser, arXiv:hep-ph/0211134.

[42] C. Giunti and M. Laveder, arXiv:hep-ph/0310238.

[43] Y. Ashie *et al.* [Super-Kamiokande Collaboration], Phys. Rev. Lett. **93**, 101801 (2004) [arXiv:hep-ex/0404034].

[44] M. Apollonio *et al.*, Eur. Phys. J. C **27**, 331 (2003) [arXiv:hep-ex/0301017].

[45] Q. R. Ahmad *et al.* [SNO Collaboration], Phys. Rev. Lett. **89**, 011301 (2002) [arXiv:nucl-ex/0204008].

[46] J. N. Bahcall, M. H. Pinsonneault and S. Basu, Astrophys. J. **555**, 990 (2001) [arXiv:astro-ph/0010346].

[47] T. Araki *et al.* [KamLAND Collaboration], arXiv:hep-ex/0406035.

[48] M. C. Gonzalez-Garcia and C. Pena-Garay, Phys. Rev. D **68**, 093003 (2003) [arXiv:hep-ph/0306001].

[49] B. Armbruster *et al.* [KARMEN Collaboration], Phys. Rev. D **65**, 112001 (2002) [arXiv:hep-ex/0203021].

[50] P. Astier *et al.* [NOMAD Collaboration], Phys. Lett. B **570**, 19 (2003) [arXiv:hep-ex/0306037].

[51] Y. Declais *et al.*, Nucl. Phys. B **434**, 503 (1995).

[52] I. E. Stockdale *et al.*, Phys. Rev. Lett. **52**, 1384 (1984).

[53] F. Dydak *et al.*, Phys. Lett. B **134**, 281 (1984).

[54] P. Astier *et al.* [NOMAD Collaboration], Nucl. Phys. B **611**, 3 (2001) [arXiv:hep-ex/0106102].

[55] E. Eskut *et al.* [CHORUS Collaboration], Phys. Lett. B **497**, 8 (2001).

[56] E. D. Church, K. Eitel, G. B. Mills and M. Steidl, Phys. Rev. D **66**, 013001 (2002) [arXiv:hep-ex/0203023].

[57] Y. Farzan and A. Y. Smirnov, Phys. Lett. B **557**, 224 (2003) [arXiv:hep-ph/0211341]; Y. Farzan, O. L. G. Peres and A. Y. Smirnov, Nucl. Phys. B **612**, 59 (2001) [arXiv:hep-ph/0105105].

[58] V. M. Lobashev *et al.*, Nucl. Phys. Proc. Suppl. **91**, 280 (2001); J. Bonn *et al.*, Nucl. Phys. Proc. Suppl. **91**, 273 (2001).

[59] A. Osipowicz *et al.* [KATRIN Collaboration], arXiv:hep-ex/0109033; L. Bornschein [KATRIN Collaboration], eConf **C030626**, FRAP14 (2003) [arXiv:hep-ex/0309007].

[60] S. Eidelman *et al.* [Particle Data Group Collaboration], Phys. Lett. B **592**, 1 (2004).

[61] K. N. Abazajian, Astropart. Phys. **19**, 303 (2003) [arXiv:astro-ph/0205238].

[62] G. L. Fogli, E. Lisi, A. Marrone, A. Melchiorri, A. Palazzo, P. Serra and J. Silk, Phys. Rev. D **70**, 113003 (2004) [arXiv:hep-ph/0408045].

[63] R. Foot and R. R. Volkas, Phys. Rev. Lett. **75**, 4350 (1995) [arXiv:hep-ph/9508275].

[64] G. Gelmini, S. Palomares-Ruiz and S. Pascoli, Phys. Rev. Lett. **93**, 081302 (2004) [arXiv:astro-ph/0403323]; S. Hannestad, Phys. Rev. D **70**, 043506 (2004) [arXiv:astro-ph/0403291].

[65] `http://www-boone.fnal.gov/publicpages/runplan.ps.gz`

[66] M. Sorel and J. M. Conrad, Phys. Rev. D **66**, 033009 (2002) [arXiv:hep-ph/0112214].

[67] M. Sorel, J. M. Conrad and M. Shaevitz, Phys. Rev. D **70**, 073004 (2004) [arXiv:hep-ph/0305255].

[68] A. Aguilar-Arevalo, V. Barger, J. M. Conrad, M. Shaevitz, M. Sorel, K. Whisnant, "CP violation in (3+2) sterile neutrino models," in preparation.

[69] P. Brâemaud, *Markov chains: Gibbs fields, Monte Carlo simulation, and queues*, Springer, New York, 1999.

[70] N. Metropolis, A. W. Rosenbluth, M. N. Rosenbluth, A. H. Teller and E. Teller, J. Chem. Phys. **21**, 1087 (1953).

[71] I. Stancu *et al.* [MiniBooNE collaboration], "Technical Design Report for the 8 GeV Beam," `http://www-boone.fnal.gov/publicpages/8gevtdr_2.0.ps.gz`

[72] I. Stancu *et al.* [MiniBooNE collaboration], "Technical Design Report for the MiniBooNE Neutrino Beam," `http://www-boone.fnal.gov/publicpages/target_tdr.ps.gz`

[73] C. Moore *et al.*, "Initial Operation of the Fermilab MiniBooNE Beamline", Proceedings of the 2003 Particle Accelerator Conference, `http://accelconf.web.cern.ch/AccelConf/p03/PAPERS/TPPB013.PDF`

[74] `http://www.bartoszekeng.com/mboone/mboone.htm`

[75] L. Bugel and M. Sorel, "Magnetic Field Measurements for the MiniBooNE Prototype Horn", BooNE Technical Note 34 (2001);

[76] S. Agostinelli *et al.* [GEANT4 Collaboration], Nucl. Instrum. Meth. A **506**, 250 (2003).

[77] `http://wwwasd.web.cern.ch/wwwasd/geant4/G4UsersDocuments/Overview/html/`

[78] J. Link and J. Monroe, private communication. Publication in preparation.

[79] N. V. Mokhov, FERMILAB-FN-0628 (1995).

[80] N. V. Mokhov, K. K. Gudima, C. C. James *et al.*, FERMILAB-Conf-04/053 (2004).

[81] Y. Cho *et al.*, Phys. Rev. D **4**, 1967 (1971).

[82] I. A. Vorontsov, V. A. Ergakov, G. A. Safronov, A. A. Sibirtsev, G. N. Smirnov, N. V. Stepanov and Y. V. Trebukhovsky, "Measurement Of Inclusive Cross-Sections Pi-, Pi+, P, H-2, H-3, He-3 At Angle ITEP-85-1983

[83] J. V. Allaby *et al.*, Phys. Lett. B **30**, 549 (1969).

[84] G. J. Marmer and D. E. Lundquist, Phys. Rev. D **3**, 1089 (1971).

[85] Y. D. Aleshin, I. A. Drabkin and V. V. Kolesnikov, ITEP-80-1977

[86] HARP Collaboration, CERN-SPSC-2004-018

[87] V. V. Gachurin *et al.*, ITEP-59-1985

[88] Lykhachev, **Zh. Eksp. Teor. Fiz. 41** (1981) 39;

[89] Afonasiev, **Yad. Fiz. 47** (1988) 1656.

[90] `http://cernlib.web.cern.ch/cernlib/overview.html`

[91] S. Geer, Phys. Rev. D **57**, 6989 (1998) [Erratum-ibid. D **59**, 039903 (1999)] [arXiv:hep-ph/9712290].

[92] L. M. Chounet, J. M. Gaillard and M. K. Gillard, Phys. Rept. **4**, 199 (1972).

[93] D. Casper, Nucl. Phys. Proc. Suppl. **112**, 161 (2002) [arXiv:hep-ph/0208030].

[94] P. Lipari, M. Lusignoli and F. Sartogo, Phys. Rev. Lett. **74**, 4384 (1995) [arXiv:hep-ph/9411341].

[95] W. A. Mann *et al.*, Phys. Rev. Lett. **31**, 844 (1973).

[96] S. J. Barish *et al.*, Phys. Rev. D **19**, 2521 (1979).

[97] N. J. Baker, P. L. Connolly, S. A. Kahn, M. J. Murtagh, R. B. Palmer, N. P. Samios and M. Tanaka, Phys. Rev. D **25**, 617 (1982).

[98] D. MacFarlane *et al.*, Z. Phys. C **26**, 1 (1984).

[99] P. E. Renton, *Electroweak Interactions*, Cambridge University Press, Cambridge, 1990.

[100] E. .D. Commins, P. H. Bucksbaum, *Weak interactions of leptons and quarks*, Cambridge University Press, Cambridge, 1983.

[101] C. H. Llewellyn Smith, Phys. Rept. **3**, 261 (1972).

[102] E. A. Paschos and J. Y. Yu, Phys. Rev. D **65**, 033002 (2002) [arXiv:hep-ph/0107261].

[103] D. Rein and L. M. Sehgal, Annals Phys. **133**, 79 (1981).

[104] R. P. Feynman, M. Kislinger and F. Ravndal, Phys. Rev. D **3**, 2706 (1971).

[105] D. Rein and L. M. Sehgal, Nucl. Phys. B **223**, 29 (1983).

[106] A. Bodek and U. K. Yang, arXiv:hep-ex/0308007.

[107] M. Gluck, E. Reya and A. Vogt, Eur. Phys. J. C **5**, 461 (1998) [arXiv:hep-ph/9806404].

[108] S. Gasiorowicz, *Elementary Particle Physics*, John Wiley and Sons, New York, 1966.

[109] M. Nowakowski, E. A. Paschos and J. M. Rodriguez, arXiv:physics/0402058.

[110] D. Griffiths, *Introduction to Elementary Particles*, John Wiley and Sons, New York, 1987.

[111] K. F. Liu, S. J. Dong, T. Draper and W. Wilcox, Phys. Rev. Lett. **74**, 2172 (1995) [arXiv:hep-lat/9406007].

[112] P. E. Bosted, Phys. Rev. C **51**, 409 (1995).

[113] S. J. Barish *et al.*, Phys. Rev. D **16**, 3103 (1977).

[114] N. J. Baker *et al.*, Phys. Rev. D **23**, 2499 (1981).

[115] R. A. Smith and E. J. Moniz, Nucl. Phys. B **43**, 605 (1972) [Erratum-ibid. B **101**, 547 (1975)].

[116] J. S. Bell and C. H. Llewellyn Smith, Nucl. Phys. B **28**, 317 (1971).

[117] S. K. Singh and E. Oset, Nucl. Phys. A **542**, 587 (1992).

[118] S. Bonetti *et al.*, Nuovo Cim. A **38**, 260 (1977).

[119] J. Brunner *et al.* [SKAT Collaboration], Z. Phys. C **45**, 551 (1990).

[120] S. V. Belikov *et al.*, Yad. Fiz. **35**, 59 (1982).

[121] S. V. Belikov *et al.*, Z. Phys. A **320**, 625 (1985).

[122] D. Ashery, I. Navon, G. Azuelos, H. K. Walter, H. J. Pfeiffer and F. W. Schleputz, Phys. Rev. C **23**, 2173 (1981).

[123] I. Navon *et al.*, Phys. Rev. C **28**, 2548 (1983);

[124] I. Stancu *et al.* [MiniBooNE collaboration], "The Miniboone Detector Technical Design Report," FERMILAB-TM-2207;

[125] R. L. Imlay *et al.*, "Study of the Angular Reconstruction of Muons in MiniBooNE Using the Muon Tracker", BooNE Technical Note 99 (2003);

[126] R. L. Imlay *et al.*, "Measuring the Energy of Muons in MiniBooNE with the Cubes", BooNE Technical Note 106 (2004);

[127] H. H. Meyer, "Index of Refraction of Marcol 7", BooNE Technical Note 90 (2003);

[128] B. C. Brown *et al.* [the MiniBooNE collaboration], "Study of scintillation, fluorescence and scattering in mineral oil for the MiniBooNE neutrino detector," FERMILAB-CONF-04-282-E; *Prepared for 2004 IEEE Nuclear Science Symposium and Medical Imaging Conference (NSS / MIC), Rome, Italy, 16-22 Oct 2004*

[129] A. O. Bazarko *et al.*, "Studies of Scattering in Marcol 7 Mineral Oil", BooNE Technical Note 144 (2004);

[130] The technical specifications for the Hamamatsu R5912 photomultiplier tube can be downloaded from: `http://www.datasheetarchive.com/HamamatsuCorporation4.html`

[131] R. B. Patterson, "The PMT Charge Calculation", BooNE Technical Note 83 (2003);

[132] Y. Liu and I. Stancu, "The MiniBooNE Charge Likelihoods and Light Scattering in Michel Electron Events", BooNE Technical Note 126 (2004);

[133] Y. Liu and I. Stancu, “Toward the MiniBooNE Charge Likelihood”, BooNE Technical Note 100 (2003);

[134] I. Stancu, “The Single-PE Time Resolution with Ryan Patterson’s QT-Algorithms”, BooNE Technical Note 81 (2003);

[135] I. Stancu, “An Introduction to the Maximum Likelihood Event Reconstruction in MiniBooNE”, BooNE Technical Note 50 (2002);

[136] Y. Liu and I. Stancu, “In Situ Speed of Light Measurements at λ=400 nm and λ=440 nm”, BooNE Technical Note 125 (2004);

[137] A. Aguilar-Arevalo, “Neutrino Energy Reconstruction Studies for numu Quasi-Elastic Events”, BooNE Technical Note 97 (2003);

[138] J. L. Raaf [BooNE Collaboration], arXiv:hep-ex/0408015.

[139] Y. Liu and I. Stancu, “The Performance of the S-Fitter Particle Identification”, BooNE Technical Note 141 (2004);